

Research article

**THE LIQUID-ORDERED PHASE IN SPHINGOMYELIN-
 CHOLESTEROL MEMBRANES AS DETECTED BY THE
 DISCRIMINATION BY OXYGEN TRANSPORT (DOT) METHOD**

ANNA WISNIEWSKA^{1,2,*} and WITOLD K. SUBCZYNSKI¹

¹Department of Biophysics, Medical College of Wisconsin, Milwaukee, WI 53226, USA, ²Department of Biophysics, Faculty of Biochemistry, Biophysics and Biotechnology, Jagiellonian University, Krakow, Poland

Abstract: Membranes made from binary mixtures of egg sphingomyelin (ESM) and cholesterol were investigated using conventional and saturation-recovery EPR observations of the 5-doxylstearic acid spin label (5-SASL). The effects of cholesterol on membrane order and the oxygen transport parameter (bimolecular collision rate of molecular oxygen with the nitroxide spin label) were monitored at the depth of the fifth carbon in fluid- and gel-phase ESM membranes. The saturation-recovery EPR discrimination by oxygen transport (DOT) method allowed the discrimination of the liquid-ordered (l_o), liquid-disordered (l_d), and solid-ordered (s_o) phases because the bimolecular collision rates of the molecular oxygen with the nitroxide spin label differ in these phases. Additionally, oxygen collision rates (the oxygen transport parameter) were obtained in coexisting phases without the need for their separation, which provides information about the internal dynamics of each phase. The addition of cholesterol causes a dramatic decrease in the oxygen transport parameter around the nitroxide moiety of 5-SASL in the l_o phase, which at 50 mol% cholesterol becomes ~5 times smaller than in the pure ESM membrane in the l_d phase, and ~2 times

*Author for correspondence: Department of Biophysics, Faculty of Biochemistry, Biophysics and Biotechnology, Jagiellonian University, ul. Gronostajowa 7, 30-387 Kraków, Poland. E-mail: wisnia@mol.uj.edu.pl, tel.: +4812 664-6355, fax: +4812 664-6902

Abbreviations used: BSM – bovine brain sphingomyelin; DMPC – dimyristoylphosphatidylcholine; DPPC – dipalmitoylphosphatidylcholine; EPR – electron paramagnetic resonance; ESM – egg sphingomyelin; FOT – fast oxygen transport; l_d – liquid-disordered; l_o – liquid-ordered; PC – phosphatidylcholine; PSM – palmitoylsphingomyelin; 5-SASL – 5-doxylstearic acid spin label; SLOT – slow oxygen transport; s_o – solid-ordered; T_1 – spin-lattice relaxation time

smaller than in the pure ESM membrane in the s_o phase. The overall change in the oxygen transport parameter is as large as ~20-fold. Conventional EPR spectra show that 5-SASL is maximally immobilized at the phase boundary between regions with coexisting l_d and l_o phases or s_o and l_o phases and the region with a single l_o phase. The obtained results allowed for the construction of a phase diagram for the ESM-cholesterol membrane.

Key words: Liquid-ordered phase, Raft domain, Sphingomyelin, Cholesterol, Lipid bilayer, Spin labeling, EPR

INTRODUCTION

Rafts are membrane domains that require lipid-lipid interaction for their formation [1]. Despite the large number of papers published on them, there are still persistent doubts about many aspects of lipid rafts, including how they are defined, and their size, composition, lifetime, and biological relevance (see recent reviews [2-6]). Rafts are considered to be representative of dynamic domains and molecular complexes in the cell membrane, although they have not yet been clearly defined [2, 3, 6]. Experiments with biological membranes defined rafts as lipid domains requiring both cholesterol and sphingolipids, and also yielded two operational definitions for lipid rafts. The first deals with the constituents of the rafts. Detergent insolubility is mainly used to biochemically define raft domains in membranes [7, 8]. In fact, the hallmark of the raft-constituent molecule is that it is recovered in the light fraction after cold Triton X-100 extraction and sucrose density gradient centrifugation. This light fraction is often called the detergent-resistant membrane fraction. The second definition deals with raft requirements in cell function: depletion of either cholesterol or sphingolipid from cell membranes leads to the disappearance of the detergent-resistant fraction and the loss (or modulation) of specific membrane functions (signaling events) connected with rafts [9]. However, such biochemical approaches do not provide direct information on rafts in the membranes of living cells [10, 11]; it is necessary to know the morphology, lifetime, molecular organization, and dynamics of the raft-constituent molecules and of the raft itself in the membrane. In model membranes, Triton X-100 promotes the formation of raft domains, which suggests that the sphingolipid-rich and cholesterol-rich domains isolated from the detergent do not reliably reflect the organization of lipids in the cell membrane [12]. These problems are emphasized in the critical review by Munro [6], in which he exposes the weak points of the raft concept. Recently, Pike [13] formulated a new definition, which states that "membrane rafts are small (10-200 nm), heterogeneous, highly dynamic, sterol- and sphingolipid-enriched domains that compartmentalize cellular processes. Small rafts can sometimes be stabilized to form larger platforms through protein-protein and protein-lipid interactions." The dynamic character of rafts has also been shown in other studies [14-16]. Suzuki *et al.* [15, 16] discussed the possible

role of dynamic raft microdomains in signal transduction in the plasma membrane.

Conventional electron paramagnetic resonance (EPR) spectroscopy has already been used to identify coexisting phases in the binary mixtures of phosphatidylcholine (PC) and cholesterol, providing evidence for the existence of the liquid-ordered phase [17-19]. On the basis of early EPR work, a phase diagram was proposed for PC-cholesterol mixtures with phase boundaries drawn indicating the region where fluid phase/fluid phase separation occurs and two immiscible phases are formed. We also made an effort to better characterize raft domains using the unique abilities of the discrimination by oxygen transport (DOT) method. This saturation-recovery EPR spin-labeling method is able not only to discriminate different membrane domains but also to characterize them by the oxygen transport parameter (oxygen diffusion-concentration product) *in situ* without the need for physical separation [14, 20, 21]. The oxygen transport parameter provides useful information about the internal dynamics of each domain [20-28]. Knowledge of these properties allows us to assign unknown domains to a certain phase. It is believed that raft domains are in the liquid-ordered phase [5, 29, 30]. However, the liquid-ordered phase is poorly characterized for the region of cholesterol concentration when it coexists with either the liquid-disordered or solid-ordered phase.

Using the DOT method, we studied the behavior of molecular oxygen in binary mixtures of dimyristoylphosphatidylcholine (DMPC) and cholesterol as a function of cholesterol content (from 0 to 50 mol% cholesterol), temperature, and the location of spin labels in the membrane [22]. This is a well-defined membrane system with a well-known phase diagram [31]. In earlier studies, the phases – liquid-ordered (l_o), liquid-disordered (l_d), and solid-ordered (s_o) – were characterized in terms of their physical properties, but mainly for cholesterol concentrations for which a sole phase (l_o , l_d , or s_o) is expected [29, 32-36]. The major effort of our recent research was focused on the cholesterol concentration range for which these phases are expected to coexist [22]. We would also like to direct readers to the paper by Almeida *et al.* [37] for a terminological discussion regarding “phases” and “domains.”

In this study, we applied both saturation-recovery and conventional EPR techniques to investigate phases and their properties in the binary mixtures of egg sphingomyelin (ESM) and cholesterol as a function of cholesterol content (from 0 to 50 mol%) and temperature. For these preliminary investigations, we chose one spin label (5-doxylstearic acid spin label, 5-SASL), with the nitroxide moiety located near the polar headgroup region in the hydrocarbon core of the membrane. This is where the rigid steroid-ring structure of cholesterol is located and where we expect to see the strongest effect of cholesterol on membrane properties. We chose 5-SASL rather than 5-PC (1-palmitoyl-2-(5-doxylstearoyl)phosphatidylcholine) to avoid introducing another phospholipid to the investigated system. Previously, we showed that the stearic acid spin labels [14, 21] distribute favorably between the membrane phases and domains.

Also, the membrane properties measured with n-SASLs were practically identical to those measured with n-PC [21, 22]. The binary mixture of sphingomyelin and cholesterol has not been as extensively investigated as PC-cholesterol mixtures; however, preliminary phase diagrams have already been published. Sankaram and Thompson [38] identified phase boundaries between the l_d and $l_d + l_o$, and the $l_d + l_o$ and l_o phases for a binary mixture of bovine brain sphingomyelin (BSM) and cholesterol, and at temperatures above the phase-transition temperature. These phase boundaries only indicate regions of cholesterol concentration and temperature in which different phases exist or coexist. However, based on these investigations alone, the phases cannot be unambiguously identified; furthermore, the physical properties of different phases cannot be extracted. De Almeida *et al.* [39] investigated the phase behavior of the palmitoylsphingomyelin-cholesterol (PSM-cholesterol) binary mixture and also identified phase boundaries. In addition to the boundaries observed by Sankaram and Thompson [38], they identified the boundaries between the s_o and $s_o + l_o$ and the $s_o + l_o$ and l_o phases at temperatures below the phase-transition temperature. In our study, we were able to detect coexisting l_o and l_d phases for temperatures above the phase-transition temperature, and coexisting l_o and s_o phases for temperatures below the phase-transition temperature. We were particularly concerned with distinguishing the l_o phase from the liquid-disordered (or solid-ordered) lipids, and obtaining the physical characteristics of this phase in the presence of other phases (*in situ*, without a physical separation). We obtained values for the oxygen transport parameter (oxygen diffusion-concentration product) in these three phases, providing unique physical characteristics for each phase. This complements our previous paper [22], in which we characterized the binary mixture of DMPC and cholesterol, the simplest paradigm for the study of liquid ordered-disordered phase separation. The data obtained in these studies could be used as a reference to compare the properties of lipid phases and domains in model and biological membranes.

MATERIALS AND METHODS

Materials

Egg sphingomyelin (ESM) and cholesterol were obtained from Avanti Polar Lipids, Inc. (Alabaster, AL). 5-doxylstearic acid spin label (5-SASL) was purchased from Molecular Probes (Eugene, OR). The chemical structures of ESM, 5-SASL and cholesterol, and their approximate localizations in the lipid bilayer membrane are presented in Fig. 1.

Preparation of the ESM-cholesterol membranes

The membranes used in this study were multilamellar dispersions of ESM containing 1 mol% of 5-SASL and various amounts of cholesterol, from 0 to 50 mol%, called the overall cholesterol mole fraction (or mixing ratio). The membranes were prepared by the method given in [17]. Briefly, chloroform

solutions of ESM, 5-SASL, and cholesterol were mixed (containing 5 μmol of total lipids), the chloroform was evaporated with a stream of nitrogen gas, and the lipid film on the bottom of the test tube was thoroughly dried under reduced pressure (about 0.1 mmHg) for 12 h. A buffer solution (0.2 mL of 0.1 M borate, pH 9.5) was added to the dried lipids at 50°C and vortexed vigorously. A rather high pH was chosen to ensure that all the 5-SASL carboxyl groups were ionized in the ESM membranes [40]. The physical properties of the ESM membranes should be insensitive to pH in the range of ~5 to ~11, because the ionization of the ESM polar phosphatidylcholine headgroups does not change in this pH range [41].

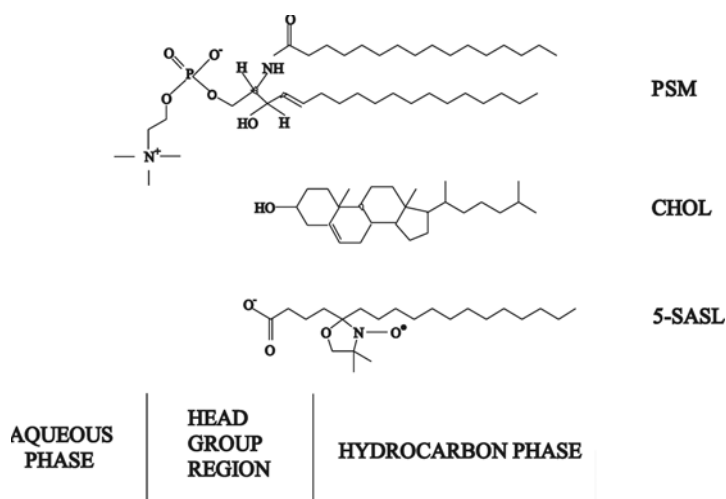


Fig. 1. The chemical structures of cholesterol, 5-SASL and PSM, and their approximate locations in the PSM bilayer. ESM is a mixture of sphingomyelins with an 84% PSM content.

Conventional EPR measurements

The ESM or ESM-cholesterol membranes were centrifuged briefly, and the loose pellet (about 20% lipid, w/w) was used for EPR measurements. The sample was placed in a capillary (0.6 mm i.d.) made of a gas-permeable polymer, TPX [42]. The capillary was placed inside the EPR dewar insert, and equilibrated with nitrogen gas, which was also used for temperature control. The sample was thoroughly deoxygenated at a temperature above the phase-transition temperature of ESM to obtain the correct line shape. In all the EPR measurements, the temperature was monitored using a copper-constantan thermocouple that was placed in the sample just above the active volume of the cavity. EPR spectra were obtained with an X-band Varian E-109 spectrometer with an E-231 Varian multipurpose cavity (rectangular TE_{102} mode).

Saturation-recovery EPR measurements

The sample was prepared like that for the conventional EPR measurements and placed in a TPX capillary (0.6 mm i.d.). For the measurements of the oxygen

transport parameter, the concentration of oxygen in the sample was controlled by equilibration with the same gas that was used for the temperature control (i.e. a controlled mixture of nitrogen and dry air adjusted with flowmeters; Matheson Gas Products, Model 7631H-604) [42, 43]. The spin-lattice relaxation times T_1 s of 5-SASL were determined by analyzing the saturation-recovery signal of the central line obtained by short-pulse saturation-recovery EPR at the X-band with the use of a loop-gap resonator [22, 27, 44, 45]. The saturation-recovery curves were fitted by single or double exponential functions.

The discrimination by oxygen transport (DOT) method

The DOT method is a dual-probe saturation-recovery EPR approach in which the observable parameter is the spin-lattice relaxation time (T_1) of lipid spin labels, and the measured value is the bimolecular collision rate between molecular oxygen and the nitroxide moiety of spin labels [20-22]. The oxygen transport parameter, $W(x)$, was introduced as a convenient quantitative measure of the rate of the collision between the spin probe and molecular oxygen by Kusumi *et al.* [28], as:

$$W(x) = T_1^{-1}(\text{Air}, x) - T_1^{-1}(\text{N}_2, x), \quad (1)$$

where the first T_1 is the spin-lattice relaxation times of the nitroxides in samples equilibrated with atmospheric air, and the second is the value for those equilibrated with nitrogen. $W(x)$ is proportional to the product of the local translational diffusion coefficient $D(x)$ and the local concentration $C(x)$ of oxygen (and is thus called a “transport” parameter) at a depth x in the membrane that is in equilibrium with atmospheric air. Thus:

$$W(x) = AD(x)C(x), \quad A = 8\pi pr_0 \quad (2)$$

where r_0 is the interaction distance between oxygen and the nitroxide moiety of the spin label (~ 4.5 Å, [46]), and p is the probability that an observable event occurs when a collision occurs; this is very close to 1 [42]. In this paper, the word “transport” is used in its basic physical sense, indicating the product of the (local) translational diffusion coefficient and the (local) concentration of oxygen in the membrane. Active transport across the membrane is not the subject of this paper.

When located in two different membrane domains or phases (e.g. the l_o and l_d , or the l_o and s_o), the spin label alone most often cannot differentiate between these domains (phases), yielding very similar (indistinguishable) conventional EPR spectra and similar T_1 values. However, even small differences in the lipid packing of these domains (phases) will affect oxygen partitioning and oxygen diffusion, which can easily be detected by observing the different T_1 s from the spin labels in these two locations in the presence of oxygen. In membranes equilibrated with air and consisting of two lipid environments with different oxygen transport rates – the fast oxygen transport (FOT) domain (phase) and the slow oxygen transport (SLOT) domain (phase) – the saturation-recovery signal

is a simple double-exponential curve with time constants of T_1^{-1} (Air, FOT) and T_1^{-1} (Air, SLOT) [14, 20, 21].

$$W(\text{FOT}) = T_1^{-1}(\text{Air, FOT}) - T_1^{-1}(\text{N}_2, \text{FOT}) \quad (3)$$

$$W(\text{SLOT}) = T_1^{-1}(\text{Air, SLOT}) - T_1^{-1}(\text{N}_2, \text{SLOT}) \quad (4)$$

Here, “x” from Eq. 1 is changed to the two membrane domains (phases), FOT and SLOT, at a fixed depth (5-SASL is distributed between the FOT and SLOT domains (phases)). $W(\text{FOT})$ and $W(\text{SLOT})$ are the oxygen transport parameters in each domain (phase), and represent the collision rates in samples equilibrated with air.

RESULTS

Saturation-recovery measurements of the oxygen transport parameter

Saturation-recovery measurements were performed for 5-SASL in ESM membranes containing various concentrations of cholesterol (from 0 to 50 mol%) and equilibrated with nitrogen or with the air/nitrogen mixture (10, 25, or 50% air in the air/nitrogen mixture). The recovery curves were fitted to single and double exponentials and compared. Fig. 2 shows the typical saturation-recovery signals for ESM membranes with 0, 20, and 50 mol% cholesterol recorded at 43°C. In the bilayers containing 0 (A, B) or 50 (E, F) mol% cholesterol, the saturation-recovery signals were satisfactorily fitted to a single exponential function in both the absence (A, E) and presence (B, F) of molecular oxygen (in nitrogen and in the mixture of 50% air and 50% nitrogen, respectively). For the overall cholesterol concentration of 20 mol% (C, D), the saturation-recovery signals in the presence of molecular oxygen (D) could be fitted satisfactorily only to double exponential curves (compare the residual for the single- and double-exponential fit), whereas a single-exponential fit was satisfactory in the absence of molecular oxygen (C). These results indicate the presence of two coexisting phases characterized by different oxygen transport parameters (the FOT and SLOT phases). As the pre-exponential factors in the fitting of the recovery curves are not robust parameters, we were unable to correlate the apparent populations of the fast- and slow-recovery components to the populations of spin labels in these two phases. The decay time constants were determined within an accuracy of $\pm 3\%$ and $\pm 5\%$, respectively for single exponential fits and double exponential fits.

The spin-lattice relaxation times (T_1 s) of 5-SASL recorded for the fluid phase ESM membranes containing cholesterol (in the absence of oxygen) were always greater than the T_1 s recorded for the pure ESM bilayer (without cholesterol). This result concurs with the theoretical development on the spin-lattice relaxation of nitroxides [47], and indicates that the motion of 5-SASL is suppressed. In our earlier work [26, 44], we also showed that cholesterol increases T_1 in and near the polar headgroup region.

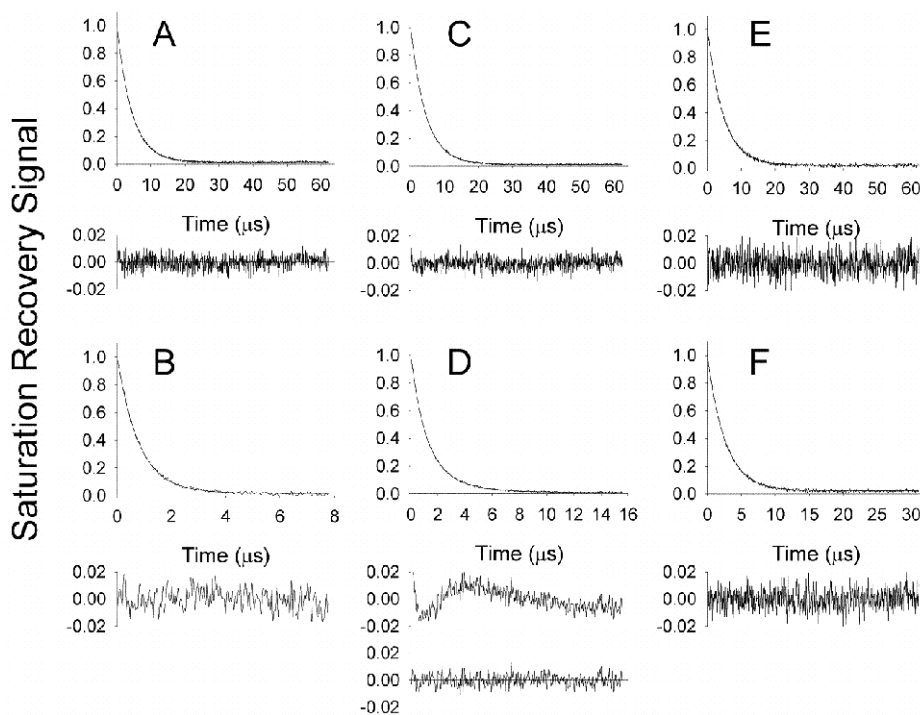


Fig. 2. Representative saturation-recovery signals with fitting curves and the residuals (the experimental signal minus the fitted curve) of 5-SASL in the ESM-cholesterol bilayer obtained at 43°C. The liposome suspensions were equilibrated with nitrogen (A, C, E) or a mixture of 50% air and 50% nitrogen (B, D, F). The overall cholesterol content (mixing ratio) in the membrane was 0 (A, B), 20 (C, D), or 50 (E, F) mol%. The experimental data was fitted either to single exponentials with time constants of 4.35 (A), 0.81 (B), 4.44 (C), 4.63 (E), and 2.65 μs (F), or to a double exponential with time constants of 2.13 and 0.93 μs (D). For 20 mol% overall cholesterol in the presence of oxygen (D), the search for a single exponential fit was unsatisfactory (see the top residual), while a double-exponential fit was excellent (see the bottom residual). The double-exponential fit is consistent with the presence of two immiscible phases (domains) with different oxygen transport parameters.

In Fig. 3, the T_1^{-1} values for 5-SASL in ESM membranes without and with 20 or 50 mol% cholesterol are shown as a function of oxygen concentration (in percent air) in the equilibrating gas mixture. All of the plots exhibited a linear dependence on the percentage of air, even when 5-SASL is distributed between two phases. This indicates that the exchange rate of 5-SASL molecules (we assume the same is valid for ESM molecules) between the two coexisting phases is slow ($<10^4 \text{ s}^{-1}$, the upper time window limit of the DOT method [20]). The oxygen transport parameter, $W(x)$, was obtained by extrapolating the linear plot to the sample equilibrated with atmospheric air (100% air, see Eq. 1 and [28]). This process is required because accurate observation of saturation

recovery is increasingly difficult, as the oxygen partial pressure increases due to faster recoveries. Not less than three decay measurements were performed for each point in the plot, with an accuracy of $W(x)$ evaluation better than $\pm 10\%$.

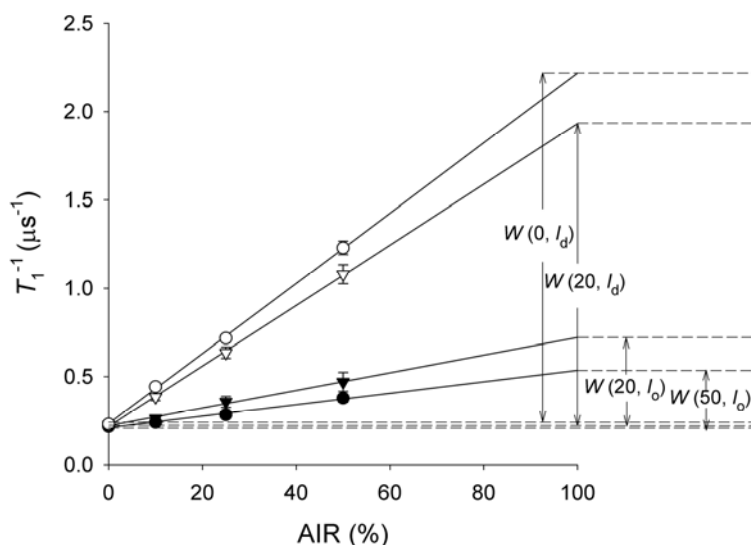


Fig. 3. T_1^{-1} for 5-SASL in various phases of the ESM-cholesterol membrane at 43°C, plotted as a function of the fraction of air in the equilibrating gas mixture. The ESM membranes were with no cholesterol (open circle, l_d phase), 20 mol% overall cholesterol (open triangle, l_d phase; solid triangle, l_o phase), and 50 mol% overall cholesterol (solid circle, l_o phase). The oxygen transport parameter (W) measured for every phase is shown. The error bars represent the maximal deviation (see the Saturation-recovery measurements of the oxygen transport parameter subsection in the Results section).

To assign the results presented in Fig. 3 (the two values of the oxygen transport parameter) to an appropriate phase or membrane domain, we used the statement from the literature that the properties of l_o phase membranes lie between those for pure phospholipid fluid (l_d) and gel (s_o) phases as a first approximation [48]. However, as we showed in our previous paper concerning the DMPC-cholesterol membrane [22], this statement is true only for low cholesterol concentrations. At high cholesterol concentrations, the properties of the l_o membrane resemble those of the gel-phase membrane in the region close to the membrane surface and those of the fluid-phase membrane in the membrane center. At temperatures lower than the phase-transition temperature, the values of the oxygen transport parameter measured in the l_o phase were even smaller than those measured in the gel-phase membrane. Therefore, we applied another criterion to our results. The properties of the l_o phase that coexists below the phase-transition temperature with the s_o phase and above the phase-transition temperature with the l_d phase should change gradually with increasing temperature and without any abrupt change at the phase transition. By contrast, the properties of the s_o phase should

change abruptly at the phase transition, because this phase disappears at higher temperatures and becomes an l_d phase. Therefore, we performed careful measurements of the temperature dependences of the oxygen transport parameter across the phase transition for the ESM membrane containing different cholesterol concentrations.

Oxygen transport parameter at phase transition

The oxygen transport parameter was measured as a function of temperature for ESM membranes containing six different overall cholesterol mole fractions (0, 10, 20, 30, 40, and 50 mol% cholesterol) in order to detect two phases (domains) existing below (s_o and l_o) and above (l_d and l_o) the phase-transition temperature of the ESM membrane. These types of plots also help to decide which data points come from the s_o , l_d , and l_o phases [22]. The data shown in Fig. 4 indicates that the lipid environment is homogenous in terms of oxygen transport (only single exponential saturation-recovery signals were observed) for the pure ESM membrane (s_o phase below and l_d phase above the phase-transition

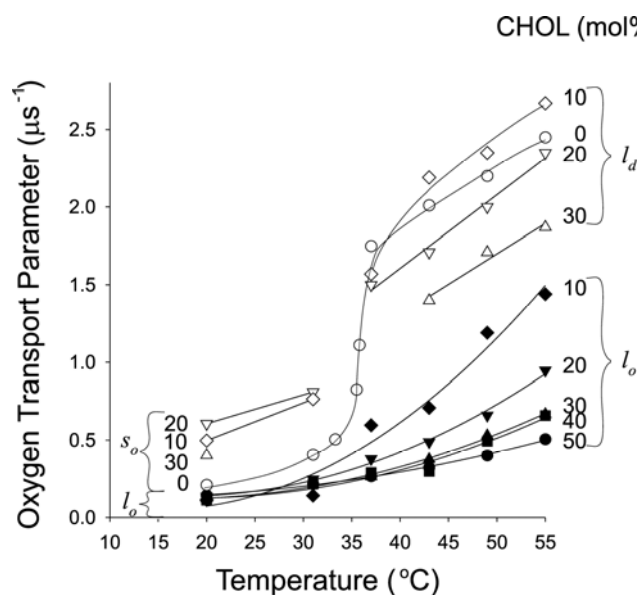


Fig. 4. The oxygen transport parameter obtained with 5-SASL in the ESM-cholesterol membrane containing 0, 10, 20, 30, 40, and 50 mol% overall cholesterol, plotted as a function of temperature. The abrupt change in oxygen transport for a pure ESM membrane observed between 33 and 37°C indicates the phase transition. The two oxygen transport parameters obtained for the membranes containing 10, 20, and 30 mol% overall cholesterol represent those for the l_o (solid symbols) and s_o (open symbols) phases below the phase-transition temperature, and l_o (solid symbols) and l_d (open symbols) phases above the phase-transition temperature of ESM. The error bars are not depicted for clarity; however, the maximal deviation of $W(x)$ was estimated as $\pm 10\%$ (see the Saturation-recovery measurements of the oxygen transport parameter subsection in the Results section).

temperature) and in the presence of 40 and 50 mol% cholesterol (l_o phase). ESM membranes with overall cholesterol mole fractions of 10, 20, and 30 mol% exhibit two coexisting phases with different oxygen transport parameters (the FOT and SLOT phases). Below the phase-transition temperature, we attribute them to the s_o and l_o phases, and above the phase-transition temperature, to the l_d and l_o phases. However, at 31 and 37°C and 30 mol% cholesterol, only one phase was found, which we attributed to the l_o phase. Points assigned to the appropriate phases are indicated in Fig. 4. As indicated above, points for which the oxygen transport parameter changes gradually across the phase transition were assigned to the l_o phase (below and above the phase-transition temperature), and points for which the oxygen transport parameter changes abruptly across the phase transition were assigned to the s_o phase below the phase-transition temperature and to the l_d phase above the phase-transition temperature. Such phase behavior (s_o turns into l_d , whereas l_o changes more gradually across the ESM membrane phase transition) was expected, and concurs with the phase diagram proposed in the Discussion. Some of the discrepancies observed for the l_o phase may be a result of the redistribution of cholesterol between coexisting s_o and l_o phases below and l_d and l_o phases above the phase-transition temperature (determined by the related phase boundaries), and/or a result of the composition of the ESM membrane, which is a mixture of sphingomyelins with an 84% PSM content.

The oxygen transport parameter in the l_o phase, at all cholesterol concentrations and at temperatures below the phase-transition temperature, is smaller by 30-50% than that in the pure gel-phase ESM membrane. Surprisingly, the oxygen transport parameter in the s_o phase at the overall cholesterol concentration of 10-30 mol% is 2-3 times greater than that in the pure gel-phase ESM membrane. Above the phase-transition temperature, the oxygen transport parameter at all cholesterol concentrations is always smaller in the l_o phase than that in the l_d phase. These are interesting and somewhat unexpected results, which will be discussed in the Discussion.

The liquid-ordered phase in a liquid-disordered or solid-ordered environment

In Fig. 5, the values of the oxygen transport parameter measured using 5-SASL incorporated into the ESM membranes are plotted as a function of the overall cholesterol content. We chose these displays to better show the properties of all the phases in the ESM-cholesterol membrane as detected by the oxygen transport parameter (oxygen diffusion-concentration product). In Fig. 5A, the values of the oxygen transport parameter in the s_o and l_d phases at different temperatures are plotted as a function of the overall cholesterol concentration. In both phases, the addition of cholesterol causes an increase of the oxygen transport parameter, with the maximal effect at 5-10 mol%. The increase is small in the l_d phase (5-8%), while in the s_o phase, the increase can be as great as 100-200%. The further addition of cholesterol causes a decrease in the oxygen transport parameter in the l_d phase (by ~30%), while the oxygen transport

parameter in the s_o phase stabilizes at the maximal level. At the overall cholesterol concentration of 10-30 mol%, both the s_o and l_d phases should be saturated with cholesterol and contain about 5 mol% cholesterol (see [38] and the phase diagram in Fig. 8). The increase in the fluidity of the s_o and l_d phases caused by such a small amount of cholesterol is in agreement with our earlier observations that small amounts of cholesterol (<5 mol%) increase the mobility of the alkyl chain (*gauche-trans* isomerization) in the gel-phase and fluid-phase dipalmitoyl-PC (DPPC) membranes [49]. In both membranes, a strong rigidifying effect of cholesterol is observed only for cholesterol concentrations above 5 mol%. The fluidizing effect was very strong in the gel-phase and rather weak in the fluid-phase membranes (see [49] for more explanation). The behavior at higher cholesterol concentrations is discussed below.

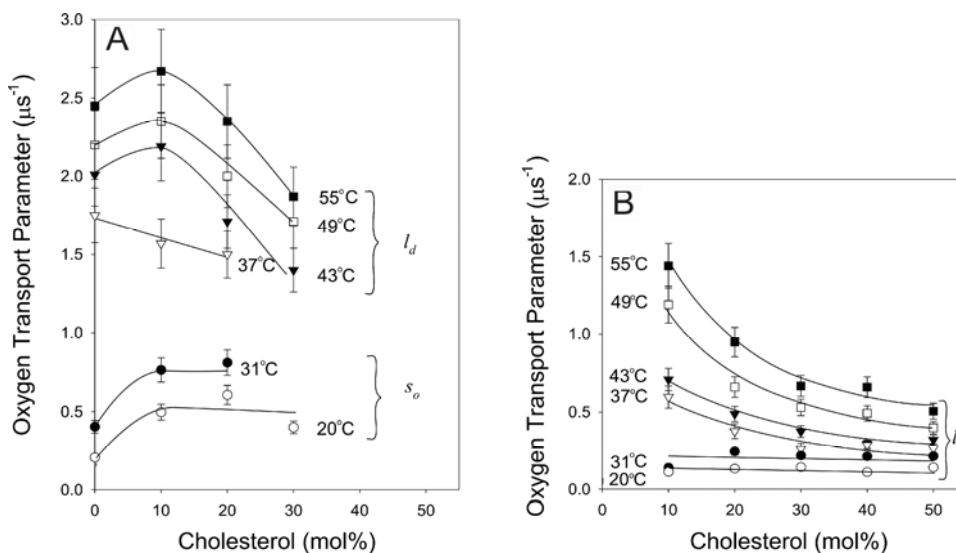


Fig. 5. The oxygen transport parameter obtained with 5-SASL in the ESM-cholesterol membrane at different temperatures, plotted as a function of the overall cholesterol concentration. A – The oxygen transport parameter in both the l_d and s_o phases. B – The oxygen transport parameter in the l_o phase. The error bars represent the maximal deviation (see the Saturation-recovery measurements of the oxygen transport parameter subsection in the Results section).

In Fig. 5B, the values of the oxygen transport parameter in the l_o phase at different temperatures are plotted as a function of the overall cholesterol concentration. All the lines drawn for the results obtained at 20-55°C are close and almost parallel, which confirms our statement that at the phase-transition temperature, the properties of the l_o phase do not abruptly change. Some discrepancy observed at low cholesterol concentrations can be explained by the different redistribution of cholesterol molecules between phases after the melting of the s_o phase at the phase transition. Additionally, the values of the oxygen

transport parameter measured at 20 and 31°C do not change with cholesterol concentration in the two coexisting phases (l_o and s_o), which is expected for a membrane made of the binary lipid mixture. According to the phase diagram in Fig. 8, variation of the overall cholesterol content between ~10 and ~30 mol% will affect only a fraction of the l_o and s_o phases, not their compositions (at 20°C, these two phases respectively contain a constant mole fraction of 35 mol% and 5 mol% cholesterol, and at 31°C, they respectively contain a constant mole fraction of 25 mol% and 5 mol% cholesterol). In the overall cholesterol mole fractions between 0 and ~5 mol% and ~30 and 50 mol%, the phases remain s_o and l_o , respectively, and the cholesterol mole fraction in both phases is the same as the experimental mixing ratio.

For temperatures above the phase-transition temperature, the l_o and l_d phases show unexpected characteristics in terms of the oxygen transport parameter. Variation of the overall cholesterol content between ~10 and ~30 mol% affects the oxygen transport parameter in the coexisting l_o and l_d phases, but even so, their compositions should not change for these cholesterol concentrations. In both phases, the oxygen transport parameter decreases when the overall cholesterol mole fraction increases. This effect suggests that when coexisting with the l_d phase, the l_o -phase domain is small. In this cholesterol range, not only do changes in the relative amounts of the l_o and l_d phases occur, but the size of the individual l_o -phase domain also increases, reducing the effects of the surrounding l_d phase. Below the phase-transition temperature, the effect of the surrounding s_o phase on the properties of the l_o phase is negligible, possibly because of its rigid and stable structure.

As shown in Figs 4 and 5, the saturation-recovery DOT method indicates the temperature and cholesterol concentration regions at which two phases coexist in the ESM-cholesterol membrane or at which the membrane exists as a single homogenous phase. The two coexisting phases were detected and characterized by the values of the oxygen transport parameter without the need for their physical separation. Our results indicate that the oxygen transport parameter is a useful monitor of membrane fluidity that reports on the translational diffusion of small molecules, and clearly show that the properties of the membrane phases monitored by the oxygen transport parameter depend on the overall cholesterol content in ESM-cholesterol membranes. It is easy to explain this dependence for regions of the phase diagram in which single homogenous phases exist as an effect of the increased cholesterol mole fraction in the l_d or s_o phase (for 0-5 mol% cholesterol) and in the l_o phase (for 30-50 mol% cholesterol). The best monitor of these changes in the l_o phase would be the profile of the oxygen transport parameter across the l_o phase membranes. In membranes made of a binary mixture of phospholipids and cholesterol, these profiles changed from the bell shape at 30 mol% cholesterol, to the rectangular shape at 50 mol% cholesterol [22, 50, 51]. It is significant to note that the abrupt increase in the oxygen transport parameter, by a factor of 2-3, which is observed at 50 mol% cholesterol, occurs between the C9 and C10 position, which is approximately

where the steroid ring structure of the cholesterol molecule reaches into the membrane. For an overall cholesterol content between 10 to 30 mol%, when two phases coexist, we explain changes in the properties of the l_o phase monitored by the oxygen transport parameter as the influence of the surrounding phases (l_d or s_o phases) caused either by the bulk effect of the surrounding phase (with different oxygen concentrations) or by the different properties of the domain boundaries. As indicated above, in either case, the data suggests that the l_o -phase domain is small (see also the discussion in [22]).

Localization of phase boundaries as detected using the conventional EPR spectra of 5-SASL

We performed additional measurements using conventional EPR techniques, which allow us to indicate the temperatures and cholesterol concentrations at which the phase boundaries in the ESM-cholesterol membrane are located. The values of the 5-SASL maximum splitting spectral parameter (indicated in Fig. 6 as $2A_{\max}$) plotted as a function of a mole fraction of cholesterol at the same temperature in fluid-phase PC-cholesterol membranes (DMPC-, DPPC-, and distearoyl-PC-cholesterol membranes) showed the extremum (the maxima in outermost splitting). The cholesterol content that yielded the largest $2A_{\max}$ increased as the temperature was raised, and the positions of the maxima (in the temperature/cholesterol mole fraction display) coincided with the boundary between the region of coexisting $l_d + l_o$ phases and the region of the l_o phase alone ([17] and citations therein). Because of the structural similarities, it seems appropriate that 5-SASL is a probe of alkyl chain order and phospholipid motion; thus, phospholipid alkyl chains are more immobilized along the boundary. A similar approach was used by Sankaram and Thompson [38] for studies on BSM-cholesterol membranes and Collado *et al.* [52] for studies on PSM-cholesterol membranes. They also found that the maximum splitting spectral parameter of 5-SASL (or 5-doxyphosphatidylcholine spin label) shows a maximum when plotted as a function of the cholesterol mole fraction and assumed that the position of this maximum indicates boundaries between appropriate regions in the BSM-cholesterol (or PSM-cholesterol) membrane phase diagram. Here, based on the conventional EPR spectra of 5-SASL in ESM-cholesterol membranes (Fig. 6), we measured the maximum splitting spectral parameter and plotted it as a function of temperature (Fig. 7A) and the cholesterol mole fraction (Fig. 7B).

Fig. 6 shows typical conventional EPR spectra of 5-SASL introduced into an ESM membrane containing different concentrations of cholesterol. $2A_{\max}$ values were used as a conventional parameter to monitor the motional freedom of the nitroxide moiety of this spin probe. In the fluid-phase membrane, these spectra can be analyzed by the method of Hubbell and McConnell [53], in which the $2A_{\max}$ is directly related to the order parameter of 5-SASL [54]. The $2A_{\max}$ value increases with increasing alkyl chain order. Usually, for brevity, this observation is described as a decrease in 5-SASL mobility. The remarkable feature of these

spectra is that there is no indication of the clearly visible conventional characteristics for the presence of two components at any temperature and at any cholesterol concentration used. This indicates that conventional EPR spectra cannot discriminate between the two coexisting phases in the ESM-cholesterol membrane (see the EPR spectra for 20 mol% cholesterol in Fig. 6B, recorded at conditions where the l_o and l_d phases or the l_o and s_o phases should coexist).

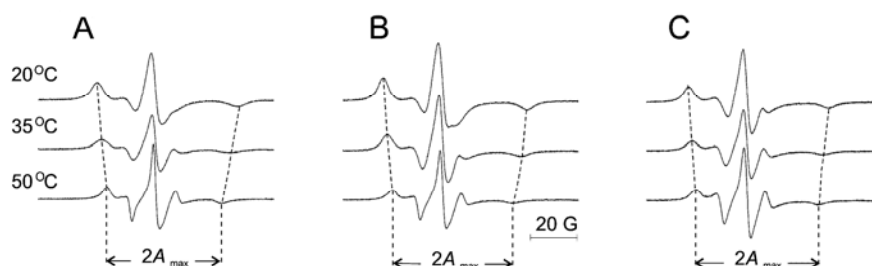


Fig. 6. EPR spectra of 5-SASL in an ESM-cholesterol membrane containing 0 (A), 20 (B), and 50 (C) mol% cholesterol, obtained at three different temperatures. The measured maximum splitting spectral parameter, $2A_{\max}$, is shown. The outer wings were also magnified by recording at a 10-fold higher receiver gain, which allowed us to measure the $2A_{\max}$ value with an accuracy better than ± 0.2 G.

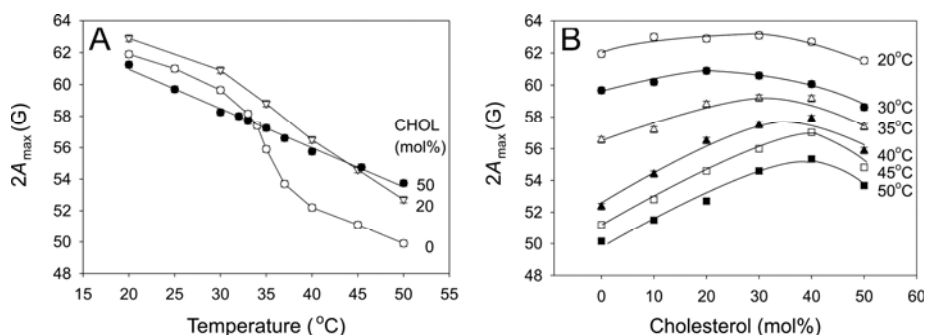


Fig. 7. The $2A_{\max}$ of 5-SASL in the ESM-cholesterol membrane containing 0, 20, and 50 mol% cholesterol, plotted as a function of temperature (A), and in the ESM-cholesterol membrane at six different temperatures, plotted as a function of cholesterol concentration (B). The error bars represent the maximal deviation (see the caption for Fig. 6).

Similarly, Kusumi *et al.* [17] and Sankaram and Thompson [38] observed single-component EPR spectra, respectively in the two-phase regions of the PC-cholesterol and BSM-cholesterol systems. We are aware that proving the absence of a second component (a strongly immobilized component) in conventional EPR spectra is difficult. As we showed previously [14, 21, 22] and confirmed here, the oxygen transport parameter obtained from the saturation-recovery measurements is a better monitor for distinguishing different membrane domains (phases) when the lifetime of the domains (phases) is longer than $\mathcal{W}(x)^{-1}$.

Fig. 7A shows that in ESM membranes containing different amounts of cholesterol, the $2A_{\max}$ of 5-SASL decreases with temperature, indicating a decrease in the alkyl chain order. In the pure ESM membrane, an abrupt change in $2A_{\max}$ values between 33 and 37°C is observed, which corresponds to the phase-transition temperature of ESM reported by Koynova and Caffrey [55]. The addition of 20 or 50 mol% cholesterol eliminates the phase transition as observed by $2A_{\max}$, although a significant difference between the effects of these two concentrations of cholesterol can be noticed, indicating that the plot of $2A_{\max}$ as a function of cholesterol content should show the extremum. Indeed, Fig. 7B shows that the $2A_{\max}$ of 5-SASL increases with the increase in cholesterol concentration up to 20-40 mol%, depending on temperature. Above this concentration, $2A_{\max}$ decreases, showing a clear maximum not only for temperatures above the phase-transition temperature, but also below that temperature. Following the observations of Kusumi *et al.* [17] and Sankaram and Thompson [38], we assume that the maximal values indicate the phase boundary. Below the phase-transition temperature, the observed boundary is between the region of $s_o + l_o$ and l_o , and above the phase-transition temperature, the boundary is between the region of $l_d + l_o$ and l_o . Similar observations were made by Sankaram and Thompson [38] for BSM-cholesterol membranes and by Collado *et al.* [52] for PSM-cholesterol membranes.

DISCUSSION

Based on saturation-recovery and conventional EPR measurements, we proposed a phase diagram for the ESM-cholesterol membrane (Fig. 8), in which we indicate three regions: Region I with coexisting l_d and l_o phases (above the phase-transition temperature), Region II with coexisting s_o and l_o phases (below the phase-transition temperature), and Region III with the single l_o phase. The boundaries between Regions I and III and Regions II and III were drawn based on measurements of the oxygen transport parameter. The horizontal bars in Fig. 8 connect the points for which two coexisting phases were observed (l_d and l_o or s_o and l_o) with the closest point for which the single l_o phase was observed (taken from Figs 4 and 5). The positions of the maxima in the $2A_{\max}$ of 5-SASL (taken from Fig. 7B) are also included, indicated by "x", and they coincide well with the boundaries drawn based on the saturation-recovery measurements. The boundary between Regions I and II was drawn based on the measurement of the phase-transition temperature, which is indicated as a vertical bar and reflects the measured width of transition (34-36°C).

Sankaram and Thompson [38] show another phase boundary in Region I at low cholesterol concentrations (about 5 mol% for temperatures close to the phase-transition temperature), namely a boundary between the l_d phase and the region of

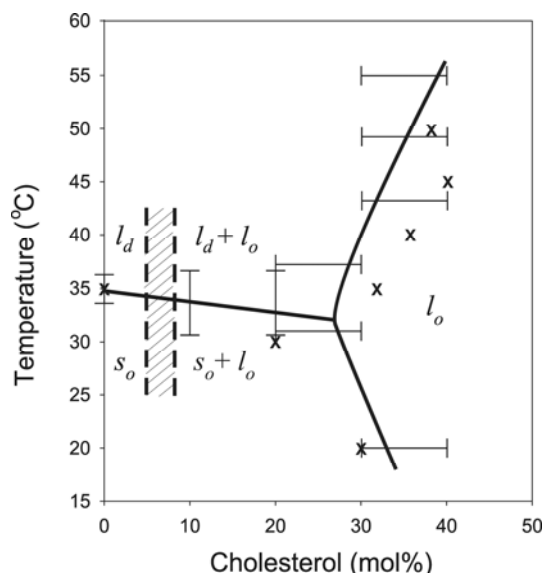


Fig. 8. The phase diagram for the ESM-cholesterol membrane. The horizontal bars were drawn based on saturation-recovery EPR measurements. They connect the point for which two coexisting phases were observed (l_d and l_o or s_o and l_o) with the closest point for which the single l_o phase was observed (taken from Figs 4 and 5). The thick lines crossing these bars represent the boundaries between these phases. The hatched area confined by vertical dotted lines represents approximate boundaries between the pure l_d phase and the region of the coexisting l_o and l_d phases, and between the pure s_o phase and the region of the coexisting l_o and s_o phases (based on de Almeida *et al.* [39] and Collado *et al.* [52]). The “x” represent the positions of the maxima in the $2A_{\max}$ of 5-SASL (from Fig. 7B) and the phase-transition temperature of the pure ESM membrane (from Fig. 7A).

the coexisting l_o and l_d phases. On the other hand, in the phase diagram drawn for PSM-cholesterol membranes by de Almeida *et al.* [39], similar boundaries between the l_d phase and the region of the coexisting l_o and l_d phases and between the s_o phase and the region of the coexisting l_o and s_o phases are indicated at slightly higher cholesterol concentrations (about 10 mol% and 8 mol%, respectively). Also, Collado *et al.* [52] discriminated these boundaries for a cholesterol concentration of about 8 mol%. Based on this information, we indicated these boundaries in a very approximate manner for temperatures close to the phase-transition temperature of ESM (Fig. 8, the hatched area confined by vertical dotted lines).

The values of the oxygen transport parameter in the l_o phase of the ESM-cholesterol membrane were obtained for the three distinct regions of the phase diagram when the l_o and l_d phases and the l_o and s_o phases coexist, and when the whole membrane was in the l_o phase. In every case, the l_o phase is characterized by low values of the oxygen transport parameter. The lowest values of the oxygen transport parameter were measured at high overall cholesterol concentrations (40 and 50 mol%). At these cholesterol concentrations

(membrane in the homogenous l_o phase), the oxygen transport parameter, when measured at the same temperature, is about 5 times smaller than in the pure ESM membrane in the l_d phase and about 2 times smaller than in the pure ESM membrane in the s_o phase. For intermediate overall cholesterol concentrations, the oxygen transport parameter in the l_o phase is about 2-3 times smaller than in the surrounding l_d phase and about 3 times smaller than in the surrounding s_o phase.

The results obtained for the ESM-cholesterol membrane differ somewhat from those obtained by us earlier for the DMPC-cholesterol membrane using the same DOT method [22]. The respective values of the oxygen transport parameter in the l_o phase of the ESM-cholesterol membrane are smaller than those in the l_o phase of the DMPC-cholesterol membrane, which indicates that the l_o phase of the former membrane is less fluid than that of the latter membrane. This can be explained by the molecular differences between sphingomyelins and phosphatidylcholines, which affect the phospholipid-cholesterol interaction. It is accepted that cholesterol interacts more strongly with sphingomyelins as compared to PC under matched conditions [56]. It has been suggested that direct intermolecular hydrogen bonding takes place between the 3β -hydroxyl group of cholesterol and the amide group of ESM [34], which may stabilize the sphingomyelin-cholesterol interaction. Also, Guo *et al.* [57] suggested that cholesterol may hydrogen-bond to the amide of sphingomyelin at higher cholesterol concentrations. It has also been shown that cholesterol condenses sphingomyelin monolayers more tightly and desorbs from such monolayers more slowly compared to PC [58], and also oxidizes more slowly in sphingomyelin bilayers when exposed to oxidase [59]. Such a strong interaction between cholesterol and sphingomyelin may be responsible for the unique properties of the l_o phase in the binary systems presented in this paper.

Acknowledgements. This study was supported by grants EY015526, EB002052, and EB001980 of the National Institutes of Health, Bethesda, MD, USA.

REFERENCES

1. Simons, K. and Ikonen, E. Functional rafts in cell membranes. **Nature** 387 (1997) 569-572.
2. Shaikh, S.R. and Edidin, M.A. Membranes are not just rafts. **Chem. Phys. Lipids** 144 (2006) 1-3.
3. Kusumi, A., Koyama-Honda, I. and Suzuki, K. Molecular dynamics and interactions for creation of stimulation-induced stabilized rafts from small unstable steady-state rafts. **Traffic** 5 (2004) 213-230.
4. Mayor, S. and Rao, M. Rafts, scale dependent, active lipid organization at the cell surface. **Traffic** 5 (2004) 231-240.
5. Edidin, M. The state of lipid rafts from model membranes to cells. **Annu. Rev. Biophys. Biomol. Struct.** 32 (2003) 257-283.

6. Munro, S. Lipid rafts: delusive or illusive. **Cell** 115 (2003) 377-388.
7. Brown, D.A. and London, E. Structure and function of sphingolipid- and cholesterol-rich membrane rafts. **J. Biol. Chem.** 275 (2000) 17221-17224.
8. Brown, D.A. and Rose, J.K. Sorting of GPI-anchored proteins to glycolipid-enriched membrane subdomains during transport to the apical cell surface. **Cell** 68 (1992) 533-544.
9. Ridgway, N.D. Interaction between metabolism and intracellular distribution of cholesterol and sphingomyelin. **Biochim. Biophys. Acta** 1484 (2000) 129-141.
10. Pralle, A., Keller, P., Florin, E.L., Simons, K. and Horber, J.K.H. Sphingolipid-cholesterol rafts diffuse as small entities in the plasma membrane of mammalian cells. **J. Cell Biol.** 148 (2000) 997-1008.
11. Friedrichson, T. and Kurzchalia, T.V. Microdomains of GPI-anchored proteins in living cells revealed by crosslinking. **Nature** 394 (1998) 802-805.
12. Heerklotz, H. Triton promotes domain formation in lipid raft mixtures. **Biophys. J.** 83 (2002) 2693-2701.
13. Pike, L.J. Rafts defined: a report on the Keystone symposium on lipid rafts and cell function. **J. Lipid Res.** 47 (2006) 1597-1598.
14. Kawasaki, K., Yin, J.-J., Subczynski, W.K., Hyde, J.S. and Kusumi, A. Pulse EPR detection of lipid exchange between protein-rich raft and bulk domains in the membrane: Methodology development and its application to studies of influenza viral membrane. **Biophys. J.** 80 (2001) 738-748.
15. Suzuki, K.G.N., Fujiwara, T.K., Sanematsu, F., Iino, R., Edidin, M. and Kusumi, A. GPI-anchored receptor clusters transiently recruit Lyn and G α for temporary cluster immobilization and Lyn activation: single-molecule tracking study 1. **J. Cell Biol.** 177 (2007) 717-730.
16. Suzuki, K.G.N., Fujiwara, T.K., Edidin, M. and Kusumi, A. Dynamic recruitment of phospholipase C γ at transiently immobilized GPI-anchored receptor clusters induces IP $_3$ -Ca $^{+2}$ signaling: single-molecule tracking study 2. **J. Cell Biol.** 177 (2007) 731-742.
17. Kusumi, A., Subczynski, W.K., Pasenkiewicz-Gierula, M., Hyde, J.S. and Merkle H. Spin-label studies on phosphatidylcholine-cholesterol membranes: effects of alkyl chain length and unsaturation in the fluid phase. **Biochim. Biophys. Acta** 854 (1986) 307-317.
18. Recktenwald, D.J. and McConnell, H.M. Phase equilibria in binary mixture of phosphatidylcholine and cholesterol. **Biochemistry** 20 (1981) 4505-4510.
19. Shimshick, E.J. and McConnell, H.M. Lateral phase separation in phospholipid membranes. **Biochemistry** 12 (1973) 2351-2360.
20. Subczynski, W.K., Widomska, J., Wisniewska, A. and Kusumi, A. Saturation recovery EPR discrimination by oxygen transport (DOT) method for characterizing membrane domains. in: **Methods in Molecular Biology. Vol. 398. Lipid Rafts.** (McIntosh, T.J., Ed.), Humana Press Inc., Totowa, New York, 2007, 145-160.

21. Ashikawa, I., Yin, J.-J., Subczynski, W.K., Kouyama, T., Hyde, J.S. and Kusumi, A. Molecular organization and dynamics in bacteriorhodopsin-rich reconstituted membranes: Discrimination of lipid environments by the oxygen transport parameter using a pulse ESR spin-labeling technique. **Biochemistry** 33 (1994) 4947-4952.
22. Subczynski, W.K., Wisniewska, A., Hyde, J.S. and Kusumi, A. Three-dimensional dynamic structure of the liquid-ordered domain as examined by a pulse-EPR oxygen probing. **Biophys. J.** 92 (2007) 1573-1584.
23. Subczynski, W.K., Pasenkiewicz-Gierula, M., McElhaney, R.N., Hyde, J.S. and Kusumi, A. Molecular dynamics of 1-palmitoyl-2-oleoylphosphatidylcholine membranes containing transmembrane α -helical peptides with alternating leucine and alanine residues. **Biochemistry** 42 (2003) 3939-3948.
24. Subczynski, W.K., Lewis, R.N.A.H., McElhaney, R.N., Hodges, R.S., Hyde, J.S. and Kusumi, A. Molecular organization and dynamics of 1-palmitoyl-2-oleoylphosphatidylcholine bilayers containing a transmembrane α -helical peptide. **Biochemistry** 37 (1998) 3156-3164.
25. Subczynski, W.K., Hopwood, L.E. and Hyde, J.S. Is the mammalian cell plasma membrane a barrier to oxygen transport? **J. Gen. Physiol.** 100 (1992) 69-87.
26. Subczynski, W.K., Hyde, J.S. and Kusumi, A. Effect of alkyl chain unsaturation and cholesterol intercalation on oxygen transport in membranes: a pulse ESR spin labeling study. **Biochemistry** 30 (1991) 8578-8590.
27. Subczynski, W.K., Hyde, J.S. and Kusumi, A. Oxygen permeability of phosphatidylcholine-cholesterol membranes. **Proc. Natl. Acad. Sci. USA** 86 (1989) 4474-4478.
28. Kusumi, A., Subczynski, W.K. and Hyde, J.S. Oxygen transport parameter in membranes as deduced by saturation recovery measurements of spin-lattice relaxation times of spin labels. **Proc. Natl. Acad. Sci. USA** 79 (1982) 1854-1858.
29. Ge, M., Field, K.A., Aneja, R., Holovka, D., Baird, B. and Freed J.H. Electron spin resonance characterization of liquid ordered phase of detergent-resistant membranes from RBL-2H3 cells. **Biophys. J.** 77 (1999) 925-933.
30. London, E. Insights into lipid raft structure and formation from experiments in model systems. **Curr. Opin. Struct. Biol.** 12 (2002) 480-486.
31. Almeida, P.F.F., Vaz, W.L.C. and Thompson, T.E. Lateral diffusion in the liquid phases of dimyristoylphosphatidylcholine/cholesterol bilayers: a free volume analysis. **Biochemistry** 31 (1992) 6739-6747.
32. Costa-Filho, A.J., Shimoyama, Y. and Freed, J.H. A2D-ELDOR study of the liquid ordered phase in multilamellar vesicle membranes. **Biophys. J.** 84 (2003) 2619-2633.

33. Ge, M., Gidvani, A., Brown, H.A., Holovka, D., Baird, B. and Freed, J.H. Ordered and disordered phases coexist in plasma membrane vesicles of RBL-2H3 mast cells. **Biophys. J.** 85 (2003) 1278-1288.
34. Veiga, M.P., Arrondo, J.L.R., Goni, F.M., Alonso, A. and Marsh, D. Interaction of cholesterol with sphingomyelin in mixed membranes containing phosphatidylcholine, studied by spin-label ESR and IR spectroscopies. A possible stabilization of gel-phase sphingolipid domains by cholesterol. **Biochemistry** 40 (2001) 2614-1622.
35. Wolf, C. and Chachaty, C. Compared effects of cholesterol and 7-dehydrocholesterol on sphingomyelin-glycerophospholipid bilayers studied by ESR. **Biophys. Chem.** 84 (2000) 269-279.
36. Gaffney, B.J. and Marsh, D. High-frequency, spin-label EPR of nonaxial lipid ordering and motion in cholesterol-containing membranes. **Proc. Natl. Acad. Sci. USA** 95 (1998) 12490-12493.
37. Almeida, P.F.F., Pokorny, A. and Hinderliter, A. Thermodynamics of membrane domains. **Biochim. Biophys. Acta** 1720 (2005) 1-13.
38. Sankaram, M.B. and Thompson, T.E. Interaction of cholesterol with various glycerophospholipids and sphingomyelin. **Biochemistry** 29 (1990) 10670-10675.
39. de Almeida, R.F.M., Fedorov, A. and Prieto, M. Sphingomyelin/phosphatidylcholine/cholesterol phase diagram: boundaries and composition of lipid rafts. **Biophys. J.** 85 (2003) 2406-2416.
40. Kusumi, A., Subczynski, W.K. and Hyde, J.S. Effects of pH on ESR spectra of stearic acid spin labels in membranes: probing the membrane surface. **Fed. Proc.** 41 (1982) 1394.
41. Papahadjopoulos, D. Surface properties of acidic phospholipids: Interaction of monolayers and hydrated liquid crystals with uni- and bi-valent metal ions. **Biochim. Biophys. Acta** 163 (1968) 240-254.
42. Hyde, J.S. and Subczynski, W.K. Spin-label oximetry. in: **Biological Magnetic Resonance. Vol. 8. Spin labeling: theory and applications.** (Berliner, L.J. and Reuben, J. Eds.), Plenum, New York, 1989, 399-425.
43. Subczynski, W.K., Felix, C.C., Klug, C.S. and Hyde, J.S. Concentration by centrifugation for gas exchange EPR oximetry measurements with loop-gap resonators. **J. Magn. Reson.** 176 (2005) 244-248.
44. Yin, J.J. and Subczynski, W.K. Effect of lutein and cholesterol on alkyl chain bending in lipid bilayers: a pulse electron paramagnetic resonance spin labeling study. **Biophys. J.** 71 (1996) 832-839.
45. Yin, J.J., Pasenkiewicz-Gierula, M. and Hyde, J.S. Lateral diffusion of lipids in membranes by pulse saturation recovery electron spin resonance. **Proc. Natl. Acad. Sci. USA** 84 (1987) 964-968.
46. Windrem, D.A. and Plachy, W.Z. The diffusion-solubility of oxygen in lipid bilayers. **Biochim. Biophys. Acta** 600 (1980) 655-665.
47. Robinson, B.H., Hass, D.A. and Mailer, C. Molecular dynamics in liquid: spin lattice relaxation of nitroxide spin labels. **Science** 263 (1994) 490-493.

48. Loura, L.M.S., Fedorov, A. and Prieto, M. Fluid-fluid membrane microheterogeneity: a fluorescence resonance energy transfer study. **Biophys. J.** 80 (2001) 778-788.
49. Subczynski, W.K. and Kusumi, A. Effects of very small amounts of cholesterol on gel-phase phosphatidylcholine membranes. **Biochim. Biophys. Acta** 854 (1986) 318-320.
50. Widomska, J., Raguz, M., Dillon, J., Gaillard, E.R. and Subczynski, W.K. Physical properties of the lipid bilayer membrane made of calf lens lipids: EPR spin labeling studies. **Biochim. Biophys. Acta** 1768 (2007) 1454-1465.
51. Widomska, J., Raguz, M. and Subczynski, W.K. Oxygen permeability of the lipid bilayer membrane made of calf lens lipids. **Biochim. Biophys. Acta** 1768 (2007) 2635-2645.
52. Collado, M.I., Goni, F.M., Alonso, A. and Marsh, D. Domain formation in sphingomyelin/cholesterol mixed membranes studied by spin-label electron spin resonance spectroscopy. **Biochemistry** 44 (2005) 4911-4918.
53. Hubbell, W.L. and McConnell, H.M. Molecular motion in spin-labeled phospholipids and membranes. **J. Am. Chem. Soc.** 93 (1971) 314-326.
54. Gaffney, B.J. Principal considerations for the calculation of order parameters for fatty acid or phospholipid spin labels in membranes. in: **Spin labeling: theory and applications.** (Berliner, L.J. Ed.), Academic Press, New York, 1976, 567-571.
55. Koynova, R. and Caffrey, M. Phases and phase transitions of the sphingolipids. **Biochim. Biophys. Acta** 1255 (1995) 213-236.
56. Ramstedt, B. and Slotte, J.P. Sphingolipids and the formation of sterol-enriched ordered membrane domains. **Biochim. Biophys. Acta** 1758 (2006) 1945-1956.
57. Guo, W., Kurze, V., Huber, T., Afdhal, N.H., Beyer, K. and Hamilton, J.A. A solid-state NMR study of phospholipid-cholesterol interactions: sphingomyelin-cholesterol binary systems. **Biophys. J.** 83 (2002) 1465-1478.
58. Ohvo, H. and Slotte, J.P. Cyclodextrin-mediated removal of sterols from monolayers: effects of sterol structure and phospholipids on desorption rate. **Biochemistry** 35 (1996) 8018-8024.
59. Slotte, J.P. Enzyme-catalyzed oxidation of cholesterol in mixed phospholipid monolayers reveals stoichiometry at which free cholesterol clusters disappear. **Biochemistry** 31 (1992) 5472-5477.